nature neuroscience

Fast delayed rectifier potassium current is required for circadian neural activity

Jason N Itri[1], Stephan Michel[1,2], Mariska J Vansteensel[2], Johanna H Meijer[2] & Christopher S Colwell[1]

In mammals, the precise circadian timing of many biological processes depends on the generation of oscillations in neural activity of pacemaker cells in the suprachiasmatic nucleus (SCN). The ionic mechanisms that underlie these rhythms are largely unknown. Using the mouse brain slice preparation, we show that the magnitude of fast delayed rectifier (FDR) potassium currents has a diurnal rhythm that peaks during the day. Notably, this rhythm continues in constant darkness, providing the first demonstration of the circadian regulation of an intrinsic voltage-gated current in mammalian cells. Blocking this current prevented the daily rhythm in firing rate in SCN neurons. Kv3.1b and Kv3.2 potassium channels were widely distributed within the SCN, with higher expression during the day. We conclude that the FDR is necessary for the circadian modulation of electrical activity in SCN neurons and represents an important part of the ionic basis for the generation of rhythmic output.

Almost all organisms, including humans, show daily rhythms in their behavior and physiology. In most cases, endogenous cellular networks composed of multiple circadian oscillators generate these rhythms. These oscillators provide temporal structure to an organism's physiological systems. Nearly all behavioral processes show significant daily variations. This temporal variation is important in the body's homeostatic mechanisms and has a major impact on the function of the nervous system. In mammals, the part of the nervous system that is responsible for most circadian behavior can be localized to a bilaterally paired structure in the hypothalamus known as the SCN[1]. Neurons in the SCN are intrinsic oscillators that continue to generate near 24-h rhythms in electrical activity, secretion and gene expression when isolated from the rest of the organism[2]. A key component that is responsible for the generation of these rhythms may be a molecular feedback loop that occurs in individual SCN neurons[3,4]. There is also evidence, however, that membrane excitability and/or synaptic transmission may be required for generation of the molecular oscillations[5,6]. Thus, clarifying the ionic mechanisms that interact with the molecular feedback loop is critical to understanding the generation of circadian oscillations at both cellular and molecular levels of organization[7].

It is well accepted that voltage-dependent potassium (K^+) currents are primary regulators of membrane excitability[8]. Given their role in other neuronal systems, K^+ currents are likely candidates to couple clock-related gene expression to membrane excitability and spontaneous firing rate in the SCN. K^+ currents are a large and diverse family of voltage regulators, and previous studies have characterized a number of intrinsic voltage-gated K^+ currents in SCN neurons that are likely to be important in regulating the firing rate of SCN neurons[9–12]. The possibility of diurnal or circadian modulation of these K^+ currents has not, however, been explored in any detail, nor do we understand how selective currents regulate the daily rhythm in the frequency of action potentials in SCN neurons. We became interested in examining the possible circadian regulation of a subtype of K^+ currents known as the FDR for two reasons. First, in molluskan retinal neurons, tetraethylammonium (TEA)-sensitive K^+ currents are thought to underlie the daily rhythm in electrical activity of these circadian pacemaker cells[13], and the slow delayed rectifier (SDR) current undergoes a circadian modulation[14]. Second, during the subjective day, SCN neurons show sustained discharge for hours without spike adaptation, and the FDR current may allow for this type of discharge in other neurons[15,16]. In the present study, we find that the FDR currents are under circadian regulation and that these currents are critical for controlling the rhythm in firing rate that is characteristic of SCN neurons.

RESULTS

Characterization of SDR and FDR currents

We used the whole-cell voltage clamp technique to isolate and record K^+ currents from neurons in the mouse SCN. Each of these cells was determined to be within the SCN by directly visualizing the cell's location with infrared–differential interference contrast videomicroscopy. In most cases, these images were sufficient to label a cell as being in either ventral or dorsal subregions[17]. Although these currents are present throughout the SCN, we focused on the dorsal subregion (dSCN) because this region shows more-robust circadian rhythms in the transcription of clock-related genes and electrical activity[18,19].

Every SCN neuron had SDR currents ($n = 76$). The SDR currents were isolated by subtraction ($I_{1\ mM\ TEA} - I_{20\ mM\ TEA}$; **Fig. 1a**) using a voltage step protocol[20,21] with a prepulse potential of −90 mV and test pulse potentials ranging from −80 to +50 mV (10-mV increments; **Fig. 1a**). The control artificial cerebrospinal fluid (ACSF) perfusion

[1]Department of Psychiatry and Biobehavioral Sciences, University of California Los Angeles, 760 Westwood Plaza, Los Angeles, California 90024-1759, USA. [2]Department of Neurophysiology, Leiden University Medical Center, P.O. Box 9604, 2300 RC Leiden, The Netherlands. Correspondence should be addressed to C.S.C. (ccolwell@mednet.ucla.edu).

Published online 24 April 2005; doi:10.1038/nn1448

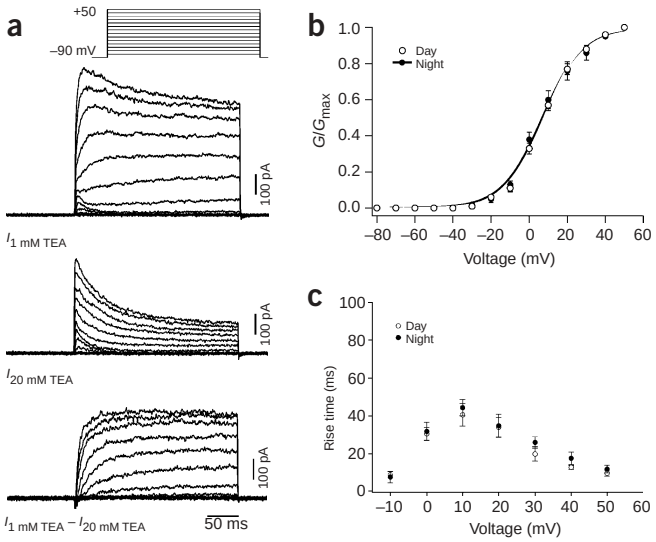

Figure 1 Characterization of SDR K^+ currents in SCN neurons. (**a**) $I_{1\ mM\ TEA}$ current traces and $I_{20\ mM\ TEA}$ current traces, which were generated after a 5-min treatment with 20 mM TEA. Bottom trace shows example of a SDR current trace isolated by subtracting $I_{20\ mM\ TEA}$ from $I_{1\ mM\ TEA}$. (**b**) Activation curves generated in dSCN neurons during the day and night by applying a hyperpolarizing prepulse (100 ms at −90 mV) followed by 900-ms voltage pulses at progressively depolarized potentials (−80 to +40 mV, 10-mV steps). (**c**) The curves show the 20–80% rise time measurements for SDR currents recorded during the day and night.

solution contained bicuculline (25 μM) to block $GABA_A$-mediated currents, TTX (0.5 μM) to block fast voltage-activated sodium channels, TEA (1 mM) or 4-aminopyridine (4-AP, 0.5 mM) to block FDR currents and cadmium (100 μM) to block calcium (Ca^{2+}) channels. The treatment ACSF solution was identical to the control solution but had 20 mM TEA to block the SDR channels. The intracellular filling solution contained BAPTA (1 mM) to buffer intracellular Ca^{2+} and inhibit Ca^{2+}-dependent K^+ currents. The SDR currents in dSCN neurons showed an activation curve with a midpoint potential of 7.7 ± 0.4 mV and steep activation characteristics (slope factor, k = 10.6 ± 0.5 mV (values are mean ± s.e.m. throughout the text); n = 7; **Fig. 1b**) during the day. The activation kinetics were similar during the night (midpoint, 6.8 ± 0.6 mV; slope factor, k = 9.9 ± 0.3 mV; n = 6; **Fig. 1b**). The 20–80% rise time was voltage dependent in dSCN neurons (ranging from 57.1 ms at 10 mV to 4.6 ms at 50 mV, n = 11; **Fig. 1c**) and was not significantly different between day and night. The current showed no inactivation during the 200-ms test pulse when measured as a ratio of current amplitude at the beginning (50 ms) and at the end of the pulse (20 mV, 1.07 ± 0.03; 30 mV, 1.01 ± 0.03; 40 mV, 0.99 ± 0.03; 50 mV, 0.93 ± 0.02; n = 17). Deactivation of SDR currents occurred with a time constant of 3.94 ± 0.35 ms (n = 10) and did not vary from day to night (day: 4.31 ± 0.62 ms, n = 5; night: 3.58 ± 0.32 ms, n = 5).

The FDR currents were also detected in every SCN neuron (n = 74), although the amplitude varied by phase. The FDR currents were isolated by subtraction ($I_{Control} - I_{4\text{-}AP}$; **Fig. 2a**) using the pulse protocol described above[21,22]. We found that 4-AP (0.5 mM) did not significantly attenuate the transient A-type K^+ current (8 ± 2% reduction, n = 8). The FDR current in dSCN neurons showed an activation curve with a midpoint potential of 6.8 ± 0.4 mV and steep activation characteristics (slope factor, k = 8.9 ± 0.4 mV; n = 9; **Fig. 2b**) during the day. The activation kinetics were similar during the night (midpoint, 7.1 ± 0.7 mV; slope factor, k = 11.6 ± 0.7 mV; n = 7; **Fig. 2b**). The 20–80% rise time was voltage dependent in dSCN neurons (ranging from 18.4 ms at 0 mV to 1.6 ms at 50 mV, n = 16; **Fig. 2c**) and was not significantly different between day and night. The current showed no inactivation during the 200-ms test pulse as characterized by the ratio of current amplitude at the beginning (50 ms) and at the end of the pulse (20 mV, 1.12 ± 0.12; 30 mV, 0.98 ± 0.03; 40 mV, 1.01 ± 0.05; 50 mV, 1.01 ± 0.04; n = 23). Deactivation of FDR currents occurred with a time constant of 2.47 ± 0.14 ms (n = 16) and did not vary from day to night (day: 2.51 ± 0.18 ms, n = 7; night: 2.38 ± 0.22 ms, n = 9). TEA (1 mM) was also used to isolate and measure FDR currents in the dSCN during the day and night. There were no differences in the kinetics and magnitude of the currents isolated with 4-AP (0.5 mM) or TEA (1 mM).

Circadian variation in FDR currents

The FDR current traces that were generated by subtraction ($I_{Control}$–$I_{4\text{-}AP}$; **Fig. 2a**) were used to determine the current-voltage relation in the dSCN during the day, the early night and the late night. The magnitude of the FDR currents was significantly greater during the day (n = 15; $P < 0.05$) than during the early night (n = 10; **Fig. 3a**) and the late night (n = 7; data not shown). The SDR current traces, which were generated by subtraction ($I_{1\ mM\ TEA} - I_{20\ mM\ TEA}$; **Fig. 1a**), were used to determine the current-voltage relation in the dSCN during day and night. There was no significant difference in the magnitude of SDR currents during the day (n = 11) as compared with those during the night (n = 9, **Fig. 3b**). To determine whether the observed rhythm in FDR currents between day and night was circadian, we carried out similar experiments on dSCN neurons from animals housed in

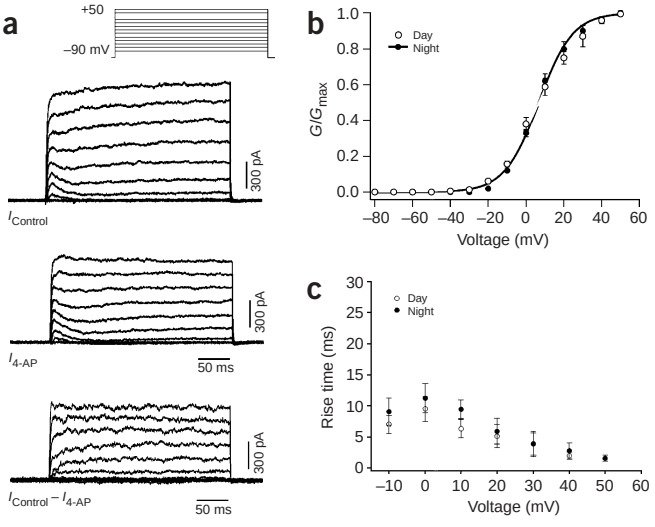

Figure 2 Characterization of FDR K^+ currents in SCN neurons. (**a**) $I_{Control}$ current traces and $I_{4\text{-}AP}$ current traces, which were generated after a 5-min treatment with 0.5 mM 4-AP. Bottom trace shows example of an FDR current trace isolated by subtracting $I_{4\text{-}AP}$ from $I_{Control}$. (**b**) Activation curves generated in dSCN neurons during the day and night by applying a hyperpolarizing prepulse (100 ms at −90 mV) followed by 900-ms voltage pulses at progressively depolarized potentials (−80 to +40 mV, 10-mV steps). (**c**) 20–80% rise time measurements for FDR currents recorded during the day and night.

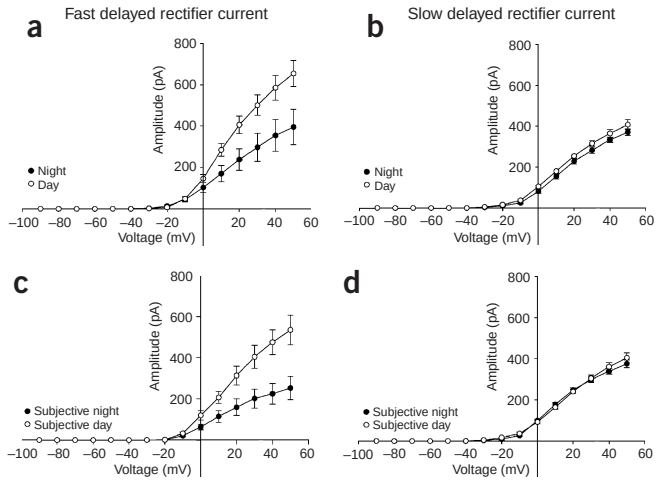

Figure 3 Current-voltage relationship of delayed rectifier K^+ currents in the mouse dSCN. (**a**) The FDR currents recorded during the day were significantly greater than those recorded during the night. (**b**) In contrast, the SDR currents did not vary between day and night. (**c**) The FDR currents recorded during the subjective day were significantly greater than those recorded during the subjective night. (**d**) The SDR currents did not vary between subjective day and night.

constant darkness (**Fig. 3c**). We found the same relationship in the magnitude of FDR currents in the dSCN between subjective day ($n = 6$; $P < 0.02$) and subjective night ($n = 6$), confirming that the rhythm is sustained in constant darkness and is endogenously generated. In contrast, there was no significant rhythm in SDR currents between subjective day ($n = 6$) and subjective night ($n = 6$; **Fig. 3d**).

Kv3.1b and Kv3.2 are expressed throughout the SCN

The Kv3.1 and Kv3.2 channels are responsible for the FDR currents[15]. To examine the pattern of expression of these channels in the SCN, we used antibodies against Kv3.1b and Kv3.2 channels (anti-Kv3.1b and anti-Kv3.2, respectively; **Fig. 4**). Mice were perfused during the day (zeitgeber time 4–6) and at night (zeitgeber time 14–16). We grouped tissue sections from each time point, and we ran immunohistochemical procedures in parallel to avoid procedural artifacts and to ensure consistency. Kv3.1b immunoreactivity was evident throughout the SCN, and most cell bodies were labeled. Staining was robust in both the dorsal and ventral regions of the SCN. This general pattern was seen throughout the rostral to caudal extent of the SCN. The mean number of immunopositive neurons per SCN section was significantly higher during the day than during the night (day: 1,941 $\pm$ 11 cells, $n = 5$; night: 59 $\pm$ 24 cells, $n = 5$; $P < 0.001$). Optical analyses of digital images of these sections indicated that the immunopositive neurons were significantly darker during the day than during the night (day, 0.42 $\pm$ 0.01 OD (optical density; see Methods); night, 0.27 $\pm$ 0.01 OD; $P < 0.001$). Anti-Kv3.2 also labeled cell bodies throughout the dorsal and ventral SCN. The staining was most robust in the rostral and central SCN regions with relatively less staining present in the caudal aspects of the nucleus. The mean number of immunopositive neurons per SCN section was also significantly higher during the day (day: 103 $\pm$ 13 cells, $n = 6$; night: 40 $\pm$ 19 cells, $n = 5$; $P < 0.02$). Again, optical density measurements indicate that the immunopositive neurons were significantly darker in the day (day, 0.37 $\pm$ 0.01 OD; night, 0.25 $\pm$ 0.01 OD; $P < 0.001$). These differences between day and night were not seen in the number (day, 80 $\pm$ 9 cells; night, 73 $\pm$ 7 cells) or optical density (day, 0.46 $\pm$ 0.02 OD; night, 0.43 $\pm$ 0.01 OD) of immunoreactive cells in the piriform cortex region of the same sections. Overall, the immunocytochemical analysis indicates that Kv3.1b and Kv3.2 channels are expressed within broad regions of the SCN and that expression of these channels is significantly higher in the day.

Regulation of spontaneous firing rate by FDR currents

Finally, we determined the contribution of FDR currents to the spontaneous firing rate (SFR) in SCN neurons with two sets of experiments. Using the current clamp recording technique in the perforated-patch configuration, we applied either 0.5 mM 4-AP or 1 mM TEA to dSCN neurons and found that blocking FDR currents reduced the mean SFR by 41 $\pm$ 4% (5.32 to 3.13 Hz; $n = 14$; $P < 0.001$; **Fig. 5a**) during the day in the presence of bicuculline (25 μM) and cadmium (100 μM). This treatment prolonged repolarization and reduced the amplitude and duration of the after-hyperpolarization of the action potential in nearly every cell treated (11 of 14; **Fig. 5b**). The reduction in SFR was long lasting and was not relieved by up to 30 min of washout ($n = 5$). Three of fourteen dSCN neurons that were recorded from during the day did not respond to treatment.

Application of 0.5 mM 4-AP or 1 mM TEA reduced the SFR of dSCN neurons during the early night by 20 $\pm$ 5% (2.80 to 2.08 Hz; $n = 13$; **Fig. 5c**). These treatments significantly lengthened repolarization and reduced the amplitude and duration of the after-hyperpolarization in most cells treated (7 of 11; **Fig. 5d**). Three of eleven dSCN neurons that were recorded from during the early night did not respond to treatment with either 4-AP or TEA. During the late night, treatment of dSCN neurons with 0.5 mM 4-AP or 1 mM TEA reduced the SFR by 9 $\pm$ 2% (2.25 to 2.08 Hz; $n = 7$; data not shown). Treatment resulted in changes to the action potential waveform that were identical to those observed during early night in nearly every cell treated (5 of 7; **Fig. 5e**,**f**). One of seven dSCN neurons that were recorded from during the late night did not respond to treatment. Overall, a comparison of all current clamp recordings from dSCN showed a significantly higher SFR during the day (5.32 Hz) than during the early night (2.80 Hz; $P < 0.001$) and during the late night (2.25 Hz; $P < 0.002$; **Fig. 6a**). After application of 0.5 mM 4-AP to eliminate the FDR current, the SFR was not

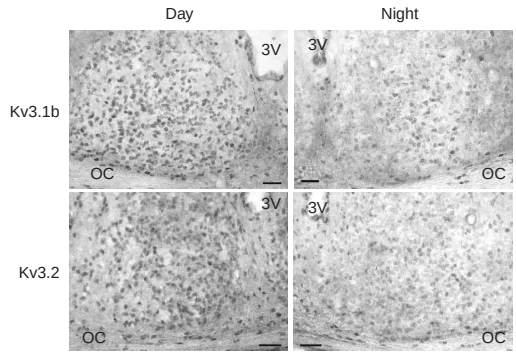

Figure 4 Photomicrographs showing immunoreactivity for Kv3.1b and Kv3.2 in the SCN during the day and night. Top panels: Kv3.1b immunoreactivity was robust throughout the SCN including the ventral lateral portions as well as a dorsal region of the SCN near the third ventricle (3V). Positive staining was seen throughout the rostral-to-caudal extent of the SCN. Bottom panels: Kv3.2 immunoreactivity was also seen on cell bodies throughout the SCN. The staining was most robust in the rostral and central aspects of the SCN. OC, optic chiasm. Scale bars, 50 μm.

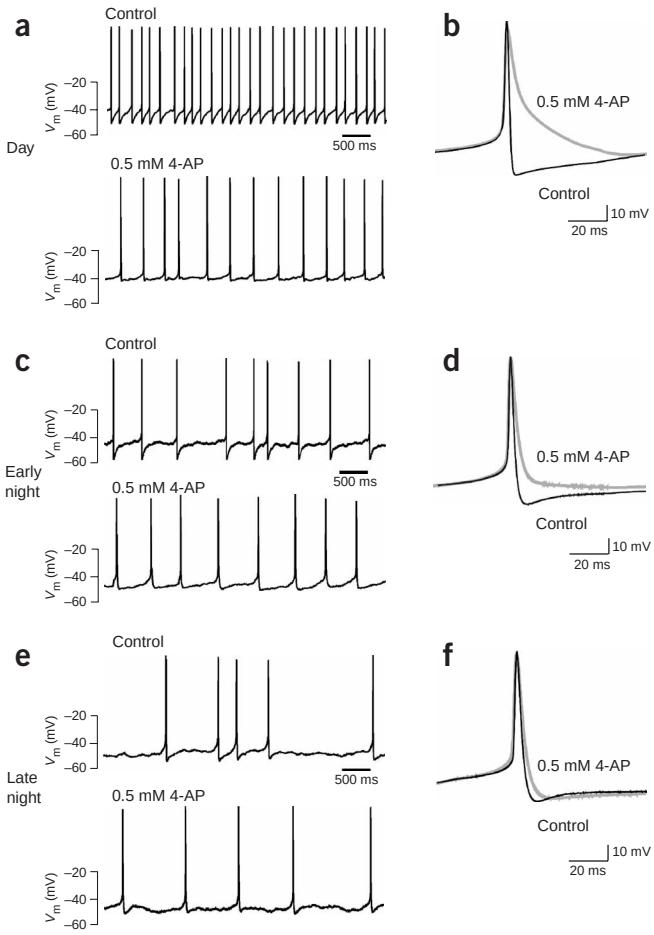

Figure 5 Blocking FDR currents significantly reduces the firing rate of SCN neurons. (**a**,**b**) Day recordings. (**c**,**d**) Early night recordings. (**e**,**f**) Late night recordings. Bath application of 0.5 mM 4-AP significantly reduced electrical activity in dSCN neurons recorded during the day, **a**, the early night, **c**, and the late night, **e**. Analysis of the average action potential waveform in **b**, **d** and **f** shows that reduction of FDR currents prolongs repolarization and reduces the magnitude of after-hyperpolarization.

significantly different between any time points ($P > 0.5$; **Fig. 6a**), indicating that the activation of the FDR was necessary for the daily modulation of neuronal activity in dSCN. Blocking the FDR current during the day resulted in a much greater reduction in SFR (41%) than during the early night (23%) or the late night (9%; **Fig. 6b**).

It is possible that blocking these K^+ channels may have a different impact on the acute firing rate of SCN neurons than it does on the longer-term circadian rhythm of the electrical activity. Therefore, in the final set of experiments, circadian rhythms of multiunit activity were recorded from mouse brain slice preparations with stationary electrodes. Data from control tissue (**Fig. 7a**,**b**) showed high activity during the middle of the projected light phase (mid–subjective day) and low activity during the projected dark phase (mid–subjective night). In contrast, this rhythm was greatly reduced or eliminated in slices treated with 0.5 mM 4-AP (**Fig. 7c**,**d**). To quantify this loss of rhythmicity, the slopes of the activity rhythm measured between zeitgeber time 23 and 4 were analyzed. The average slope of the control recordings was 34 ± 6 Hz h^{-1} ($n = 6$), whereas the 4-AP–treated slices had a slope of 1.5 ± 3 Hz h^{-1} ($n = 6$). The control slope, but not the 4-AP–treated slope, was significantly different from zero ($P < 0.01$). Furthermore, no significant positive slope was detected in 4-AP–treated slices during the whole recording as tested during six intervals (3 h) between zeitgeber time 15.5 and 9.5. At the end of the experiment, all slices showed a robust increase in firing in response to NMDA (5 μM; data not shown), indicating viability of the slice at the tissue level.

DISCUSSION

In the present study, we have used perforated and whole-cell patch electrophysiological techniques to record outward K^+ currents in SCN neurons. We provide the first description of a circadian modulation of an FDR K^+ current in SCN neurons. Two different pharmacological treatments (4-AP and TEA) were used to isolate SDR and FDR currents[21,22]. As described in other neurons, these currents activate only at depolarized membrane potentials and have rapid activation and deactivation kinetics. In the SCN, the FDR current begins to activate at −20 mV, and most neurons have half-activation voltages around 6 mV. Once activated, the fast kinetics of this current allow neurons to repolarize quickly after generation of action potentials without altering the spike threshold or action potential height[15]. These currents are found in cell populations with high firing rates in sensory[20] and motor circuits[16]. The presence of this current should allow SCN neurons to discharge at higher rates during the day without adaptation. The FDR current is sensitive to both 4-AP (0.5 mM) and TEA (1 mM), which gives us pharmacological tools to investigate the contribution of this current to the frequency of action potential generation in the SCN. Using perforated-patch recording techniques to minimize cell dialysis and obtain reliable SFR recordings[23], we have found that acutely blocking the FDR with 0.5 mM 4-AP or 1 mM TEA significantly decreases the firing rate of SCN neurons during the day so that the difference between day and night SFR was eliminated. This is an

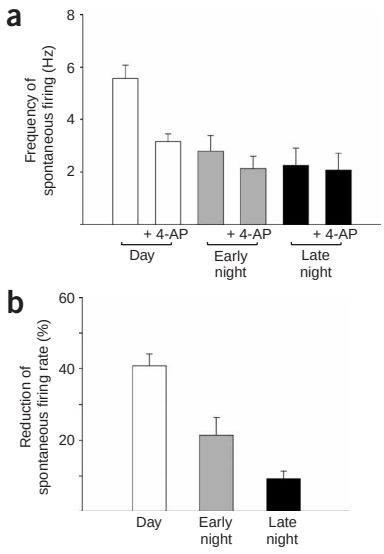

Figure 6 Acutely blocking the FDR current causes significant reduction in firing rate of SCN neurons during the day. (**a**) Effect of blocking FDR channels with 0.5 mM 4-AP during the day, early night and late night in the dSCN. Similar results were obtained with application of 1 mM TEA (data not shown). (**b**) Blocking FDR channels during the day results in a greater decrease in the SFR than does blocking channels during the early and late night.

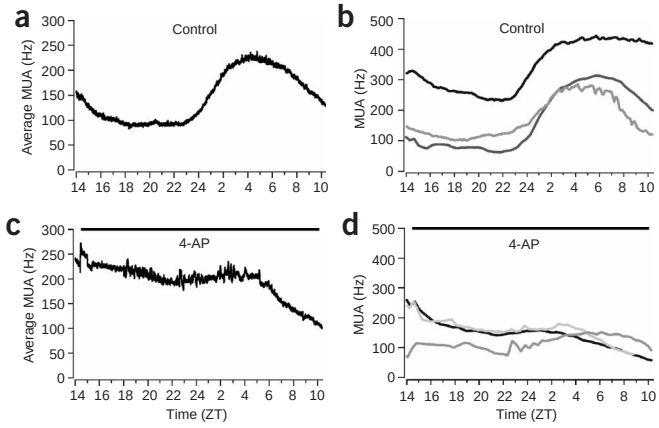

Figure 7 The daily rhythm in the SFR is lost when the FDR current is blocked. Rhythms in multiunit activity (MUA) were recorded in mouse SCN. (**a**) Control slices ($n = 6$) had an average circadian rhythm in spontaneous electrical activity with peak activity during the middle of the projected light phase (mid–subjective day) and low activity during the projected dark phase (mid–subjective night). (**b**) Representative examples of electrical activity recorded from three control SCN slices. (**c**) In contrast, this rhythm was greatly reduced or eliminated in those slices treated with 4-AP (0.5 mM; $n = 6$). (**d**) Representative examples of electrical activity recorded from three SCN slices treated with 4-AP. ZT, zeitgeber time.

unusual feature of the FDR, because blockage of most K^+ currents would be expected to increase firing rate. Finally, using extracellular recordings of rhythms in multiunit activity, we found that longer-term application of 4-AP (0.5 mM) prevented expression of diurnal rhythms in electrical activity recorded from SCN tissue.

Based on our observations, we believe that the FDR K^+ current is necessary for the expression of the circadian rhythm in the frequency of action potentials. We have found that the rhythm in the magnitude of this current is correlated with the rhythm in electrical discharge: both peak during the day and are low during the night. This rhythm in amplitude continues in constant darkness and seems to be a circadian rhythm that is expressed at the level of individual SCN neurons. Other properties of the current such as voltage dependence and activation and deactivation kinetics do not change with the daily cycle. The SDR current does not show a diurnal or circadian rhythm in amplitude or kinetic parameters in the dSCN. In addition, when the FDR is acutely blocked with 4-AP, the frequency of firing in the SCN is significantly reduced, with the largest effects occurring in dSCN neurons recorded during the day. Longer treatments of 4-AP prevented the daily rhythm of firing in the SCN. Although the evidence presented points to a crucial role of the FDR in diurnal and circadian SFR modulation, this current cannot be responsible for the initial membrane depolarization at dawn. The FDR acts only across a range of voltages that are depolarized relative to the resting membrane potential of SCN neurons. Another class of current must be responsible for driving action potential generation to activate FDR channels.

SCN neurons have a slowly inactivating sodium current, which activates around −65 mV[24,25]. Although it is not known if this current shows a circadian rhythm, blocking this sodium current inhibits spontaneous firing[25]. In addition, previous work has found evidence for a daily rhythm in an L-type calcium current[26]. These sodium and calcium currents are probably critical for moving the SCN neuron into a voltage range in which the FDR would be activated. Finally, electrophysiological measurements from SCN neurons indicate that input resistance also peaks during the day[23,27,28]. These observations indicate that when SCN neurons are at their resting membrane potential, the net current flow through ion channels is lower during the day. Because the membrane is also depolarized during the day[23], the closed channels are likely to be K^+ channels. Important support for this model comes from the observation that a TEA-sensitive K^+ current is critical for the daily change in input resistance[28]. The identity of these channels is not yet known, and these studies raise the possibility that a whole set of currents change rhythmically in the SCN as the cell moves from an 'inactive/down' state during the night to an 'active/up' state during the day. Not all currents within the SCN are rhythmically regulated, however, and the SDR current (this study), a barium-sensitive K^+ current[10] and H-currents[29] all seem to be constant from day to night.

The mechanisms that underlie the daily rhythm in FDR currents is not known. Our immunocytochemical evidence clearly indicates the presence of the Kv3.1b and Kv3.2 channels in the SCN and indicates that expression of these channel proteins may be rhythmically regulated. It is possible that the genes *Kcnc1* (also known as *Kv3.1*) and *Kcnc2* (also known as *Kv3.2*) are rhythmically regulated, as many genes in this region show transcriptional rhythms[30] and the promoter region of the *Kcnc1* contains both CRE and AP-1 sites[31]. Cells in the SCN exhibit a prominent circadian oscillation in CRE-mediated gene expression[32], and we expect to see a rhythm in the expression of the genes coding for the fDR. In *Drosophila melanogaster*, circadian rhythms in levels of mRNA coding for a regulatory protein associated with Ca^{2+}-sensitive K^+ channels have been described[33,34]. Furthermore, in mammalian cardiac tissue, diurnal variation occurs in the expression of genes that encode two K^+ channels (Kv1.5 and Kv4.2)[35]. The regulation need not be transcriptional, however, and post-translational modifications could also be responsible for the daily rhythms. Outside of the SCN, kinase and/or phosphatase activity is important for mediating short-term changes in channel function that alter electrical excitability[8]. In chick photoreceptors, circadian oscillations in cone cGMP-gated channels have been well described[36]. Within the SCN, circadian patterns of phosphorylation seem to be critical for the basic molecular feedback loop that drives circadian rhythms, with the involvement of casein kinases being particularly important[37]. Regardless of the underlying mechanism, the work described in the present study identifies a specific K^+ current that is under the regulatory control of the molecular circadian feedback loop and demonstrates that this current is necessary for the daily rhythm in frequency of action potential generation that lies at the heart of the SCN oscillator.

METHODS

In all studies, recommendations for animal use and welfare dictated by the University of California Los Angeles Division of Laboratory Animals and guidelines from the U.S. National Institutes of Health or the Animal Experiments Ethical Committee of the Leiden University Medical Center were followed.

Behavioral measurements. Male mice of at least 21 d of age were housed individually, and their wheel-running activity was recorded (Mini Mitter). Zeitgeber time is used to describe the projected time based on the previous light cycle, with lights on defined as zeitgeber time 0. Circadian time was used when mice were in constant darkness and the onset of activity was defined as circadian time 12. When necessary, mice were killed in darkness while using an infrared viewer. In all cases, mice were killed 1 h before recording.

Whole-cell patch clamp electrophysiology. Brain slices were prepared using standard techniques from mice (C57Bl/6) of 30–50 d old. Methods, including solutions, were identical to those described previously[17]. For perforated-patch recordings, a standard internal solution was used to fill the tip of the patch pipette. Amphotericin was dissolved in DMSO and was mixed with standard

internal solution at 0.2 mM for backfilling the patch pipette. Recordings were obtained with an Axon Instruments 200B amplifier and were monitored on-line with pCLAMP (Axon Instruments). To minimize changes in offset potentials with changing ionic conditions, the ground path used a KCl agar bridge. Whole-cell capacitance and electrode resistance were neutralized and compensated (50–80%). Series and input resistances were monitored repeatedly by checking the response to small pulses in a passive potential range. Series resistance was not compensated, and the maximal voltage error that was due to this resistance was calculated to be 6 mV. The access resistance of these cells was 15–35 MΩ in the whole-cell voltage clamp configuration, whereas the cell capacitance was typically 6–18 pF.

Current traces were recorded with pClamp using the whole-cell voltage clamp recording configuration and then were analyzed using ClampFit. Delayed rectifier K^+ currents were isolated pharmacologically using a voltage step protocol in the whole-cell voltage clamp configuration. The protocol consisted of a 100-ms prepulse at −90 mV followed by a 250-ms step at progressively depolarized potentials. Leak subtraction was carried out during acquisition using a p/4 protocol, which uses four subpulses with one-quarter of the test pulse amplitude and reversed polarity given from a holding potential of −70 mV. Current traces from treatments were subtracted from controls to isolate delayed rectifier currents. Both 4-AP (0.5 mM) and TEA (1 mM) were used to isolate FDR currents, whereas high-concentration TEA (20 mM) was used to isolate SDR currents. Current measurements were done in the control solution and after 5–7 min of drug treatment in each cell. Activation curves were generated using data collected from the voltage step protocol outlined above and were fit with a Boltzmann function $f(V_m) = 1/(1 + \exp[-(V_m - V_{half})/k])$, where V_m is the membrane potential, V_{half} is the membrane potential at which the value of the Boltzmann function equals 0.5 and k is the slope factor. Inactivation curves were generated by using the following protocol in the whole-cell voltage clamp configuration: 100-ms prepulses of varying potentials (−100 mV to −30 mV, 5-mV steps) followed by a 900-ms step at +50 mV to elicit maximal current. Data were fit with the Boltzmann function described for activation curves, and 20–80% rise time measurements were made on current traces. The SFR and action potential waveforms were recorded with pClamp using current clamp in the whole-cell perforated-patch configuration. No current was injected during recording. After a baseline SFR was established, drug treatment began within 5 min of obtaining the perforated-patch configuration (access resistance <100 MΩ).

Extracellular recording. The multiunit activity rhythms of SCN neurons were measured as described[38]. Coronal slices (500 μm) were prepared from male C57Bl/6 mice at the beginning of the subjective day. The slices were kept submerged with a thin fork in a laminar flow chamber (35.5 °C). Slices contained at least 50% of the rostrocaudal extent of the SCN and all of the ventrodorsal extent. Extracellular electrical activity of SCN neurons was measured by platinum/iridium electrodes and was subsequently amplified and bandwidth filtered[39]. Action potentials with a signal-to-noise ratio of 2:1 (noise <5 μV from baseline) were selected by spike triggers and were counted electronically every 10 s for about one circadian cycle. The positions of the electrodes and spike trigger settings were not changed during the experiment. Linear fits were done on the multiunit activity data between zeitgeber time 23 and 4, and the slopes of the resulting lines were determined. A significant positive slope at this circadian time is indicative of a typical rhythm in electrical activity. The obtained slopes from control and experimental slices were tested against zero using a one-sided t-test ($P < 0.05$). The individual examples in the figures were smoothed with a box filter for clearer presentation of the data.

Immunocytochemistry. The methods were similar to those previously described[40]. Polyclonal anti-Kv3.1b and anti-Kv3.2, raised in rabbit, were used (Alomone Labs). A dilution series was done for both antibodies, with optimal dilution found to be 1:150 for anti-Kv3.2 and 1:400 for anti-Kv3.1b. Anti-Kv3.1b was raised to amino acids 567–585, which is a sequence that is unique to the Kv3.1b splice variant, whereas anti-Kv3.2 recognizes a sequence that is common to all known splice variants of Kv3.2, amino acids 184–204. Tissue sections from each time point were grouped and processed in parallel to avoid procedural artifacts and to ensure consistency. Immunocytochemical controls included the omission of primary and secondary antisera and preabsorption of antibodies with appropriate peptide epitopes. We found that that the omission of primary antibodies and preabsorption with appropriate epitopes blocked all staining.

For each mouse, images were taken from one section from each of three regions (rostral, middle and caudal) using a SPOT camera system (Diagnostic Instruments). All immunopositive cells within the SCN of these three sections were counted manually at 400× with the aid of a grid. All immunopositive cells within the grid were counted without regard to the intensity of the staining. Counts were done by two observers who were blind to the treatment protocol, and the results were averaged. To have some measure of the intensity of staining, optical density measurements were also undertaken using SigmaScan Pro software (SPSS). For this analysis, digital images were converted to an 8-bit gray scale in which each pixel would register a gray level value between 0 (dark) and 255 (white). SCN neurons were manually outlined so that the program could determine the average gray level per neuron. The optical density was then calculated as OD = −log(gray level of the neuron/maximum gray level). The microscope, lighting and software parameters were held constant to allow comparisons to be made in the optical density measurements between tissue sections. Cell counts and optical density measurements were also made in the piriform cortical region of the same sections that contained the SCN.

Statistical analyses. Between-group differences were first evaluated using an analysis of variance to determine whether there were any significant differences among means of all groups. *Post hoc* pairwise comparisons were then done using t-tests or Mann-Whitney rank sum tests when appropriate. Values were considered significant if $P < 0.05$. All tests were carried out using SigmaStat (SPSS). In the text, values are shown as mean ± s.e.m.

ACKNOWLEDGMENTS

We would like to thank H. Duindam for technical assistance. We would also like to thank E. Herzog and N. Wayne for comments on a draft of the manuscript. Supported by National Institutes of Health grants HL64582, NS043169 and MH68087.

COMPETING INTERESTS STATEMENT

The authors declare that they have no competing financial interests.

Received 18 January; accepted 29 March 2005
Published online at http://www.nature.com/natureneuroscience/

1. van Esseveldt, K.E., Lehman, M.N. & Boer, G.J. The suprachiasmatic nucleus and the circadian time-keeping system revisited. *Brain Res. Brain Res. Rev.* **33**, 34–77 (2000).
2. Gillette, M.U. Cellular and biochemical mechanisms underlying circadian rhythms in vertebrates. *Curr. Opin. Neurobiol.* **7**, 797–804 (1997).
3. King, D.P. & Takahashi, J.S. Molecular genetics of circadian rhythms in mammals. *Annu. Rev. Neurosci.* **23**, 713–742 (2000).
4. Reppert, S.M. & Weaver, D.R. Molecular analysis of mammalian circadian rhythms. *Annu. Rev. Physiol.* **63**, 647–676 (2001).
5. Nitabach, M.N., Blau, J. & Holmes, T.C. Electrical silencing of *Drosophila* pacemaker neurons stops the free-running circadian clock. *Cell* **109**, 485–495 (2002).
6. Harmar, A.J. *et al.* The VPAC2 Receptor is essential for circadian function in the mouse suprachiasmatic nuclei. *Cell* **109**, 497–508 (2002).
7. Schaap, J., Pennartz, C.M. & Meijer, J.H. Electrophysiology of the circadian pacemaker in mammals. *Chronobiol. Int.* **20**, 171–188 (2003).
8. Hille, B. *Ion Channels of Excitable Membranes* (Sinauer Associates, Sunderland, Massachusetts, USA, 2001).
9. Bouskila, Y. & Dudek, F.E. A rapidly activating type of outward rectifier K^+ current and A-current in rat suprachiasmatic nucleus neurones. *J. Physiol. (Lond.)* **488**, 339–350 (1995).
10. De Jeu, M., Geurtsen, A. & Pennartz, C.M.A. Ba^{2+}-sensitive K^+ current contributes to the resting membrane potential of neurons in rat suprachiasmatic nucleus. *J. Neurophysiol.* **88**, 869–878 (2002).
11. Cloues, R.K. & Sather, W.A. Afterhyperpolarization regulates firing rate in neurons of the suprachiasmatic nucleus. *J. Neurosci.* **23**, 1593–1604 (2003).
12. Teshima, K., Kim, S.H. & Allen, C.N. Characterization of an apamin-sensitive potassium current in suprachiasmatic nucleus neurons. *Neuroscience* **120**, 65–73 (2003).
13. Michel, S., Geusz, M.E., Zaritsky, J.J. & Block, G.D. Circadian rhythm in membrane conductance expressed in isolated neurons. *Science* **259**, 239–241 (1993).
14. Michel, S., Manivannan, K., Zaritsky, J.J. & Block, G.D. A delayed rectifier current is modulated by the circadian pacemaker in Bulla. *J. Biol. Rhythms* **14**, 141–150 (1999).
15. Rudy, B. & McBain, C.J. Kv3 channels: voltage-gated K^+ channels designed for high-frequency repetitive firing. *Trends Neurosci.* **24**, 517–526 (2001).

16. Baranauskas, G., Tkatch, T., Nagata, K., Yeh, J.Z. & Surmeier, D.J. Kv3.4 subunits enhance the repolarizing efficiency of Kv3.1 channels in fast-spiking neurons. *Nat. Neurosci.* **6**, 258–266 (2003).
17. Itri, J. & Colwell, C.S. Regulation of inhibitory synaptic transmission by vasoactive intestinal peptide (VIP) in the mouse suprachiasmatic nucleus. *J. Neurophysiol.* **90**, 1589–1597 (2003).
18. Hamada, T., Antle, M.C. & Silver, R. Temporal and spatial expression patterns of canonical clock genes and clock-controlled genes in the suprachiasmatic nucleus. *Eur. J. Neurosci.* **19**, 1741–1748 (2004).
19. Yamaguchi, S. *et al.* Synchronization of cellular clocks in the suprachiasmatic nucleus. *Science* **302**, 1408–1412 (2003).
20. Wang, L.Y., Gan, L., Forsythe, I.D. & Kaczmarek, L.K. Contribution of the Kv3.1 potassium channel to high-frequency firing in mouse auditory neurones. *J. Physiol. (Lond.)* **509**, 183–194 (1998).
21. Martina, M., Schultz, J.H., Ehmke, H., Monyer, H. & Jonas, P. Functional and molecular differences between voltage-gated K^+ channels of fast-spiking interneurons and pyramidal neurons of rat hippocampus. *J. Neurosci.* **18**, 8111–8125 (1998).
22. Kirsch, G.E. & Drewe, J.A. Gating-dependent mechanism of 4-aminopyridine block in two related potassium channels. *J. Gen. Physiol.* **102**, 797–816 (1993).
23. Schaap, J. *et al.* Neurons of the rat suprachiasmatic nucleus show a circadian rhythm in membrane properties that is lost during prolonged whole-cell recording. *Brain Res.* **815**, 154–166 (1999).
24. Pennartz, C.M., Bierlaagh, M.A. & Geurtsen, A.M. Cellular mechanisms underlying spontaneous firing in rat suprachiasmatic nucleus: involvement of a slowly inactivating component of sodium current. *J. Neurophysiol.* **78**, 1811–1825 (1997).
25. Kononenko, N.I., Shao, L.R. & Dudek, F.E. Riluzole-sensitive slowly inactivating sodium current in rat suprachiasmatic nucleus neurons. *J. Neurophysiol.* **91**, 710–718 (2004).
26. Pennartz, C.M., de Jeu, M.T., Bos, N.P., Schaap, J. & Geurtsen, A.M. Diurnal modulation of pacemaker potentials and calcium current in the mammalian circadian clock. *Nature* **416**, 286–290 (2002).
27. Jiang, Z.G., Yang, Y., Liu, Z.P. & Allen, C.N. Membrane properties and synaptic inputs of suprachiasmatic nucleus neurons in rat brain slices. *J. Physiol. (Lond.)* **499**, 141–159 (1997).
28. Kuhlman, S.J. & McMahon, D.G. Rhythmic regulation of membrane potential and potassium current persists in SCN neurons in the absence of environmental input. *Eur. J. Neurosci.* **20**, 1113–1117 (2004).
29. de Jeu, M.T. & Pennartz, C.M. Functional characterization of the H-current in SCN neurons in subjective day and night: a whole-cell patch-clamp study in acutely prepared brain slices. *Brain Res.* **767**, 72–80 (1997).
30. Panda, S. *et al.* Coordinated transcription of key pathways in the mouse by the circadian clock. *Cell* **109**, 307–320 (2002).
31. Gan, L. & Kaczmarek, L.K. When, where, and how much? Expression of the Kv3.1 potassium channel in high-frequency firing neurons. *J. Neurobiol.* **37**, 69–79 (1998).
32. Obrietan, K., Impey, S., Smith, D., Athos, J. & Storm, D.R. Circadian regulation of cAMP response element-mediated gene expression in the suprachiasmatic nuclei. *J. Biol. Chem.* **274**, 17748–17756 (1999).
33. McDonald, M.J. & Rosbash, M. Microarray analysis and organization of circadian gene expression in *Drosophila*. *Cell* **107**, 567–578 (2001).
34. Ceriani, M.F. *et al.* Genome-wide expression analysis in *Drosophila* reveals genes controlling circadian behavior. *J. Neurosci.* **22**, 9305–9319 (2002).
35. Yamashita, T. *et al.* Circadian variation of cardiac K^+ channel gene expression. *Circulation* **107**, 1917–1922 (2003).
36. Ko, G.Y., Ko, M.L. & Dryer, S.E. Circadian regulation of cGMP-gated channels of vertebrate cone photoreceptors: role of cAMP and Ras. *J. Neurosci.* **24**, 1296–1304 (2004).
37. Reppert, S.M. & Weaver, D.R. Coordination of circadian timing in mammals. *Nature* **418**, 935–941 (2002).
38. Meijer, J.H., Schaap, J., Watanabe, K. & Albus, H. Multiunit activity recordings in the suprachiasmatic nuclei: in vivo versus in vitro models. *Brain Res.* **753**, 322–327 (1997).
39. Schaap, J. *et al.* Heterogeneity of rhythmic suprachiasmatic nucleus neurons: Implications for circadian waveform and photoperiodic encoding. *Proc. Natl. Acad. Sci. USA* **100**, 15994–15999 (2003).
40. Michel, S., Itri, J. & Colwell, C.S. Excitatory mechanisms in the suprachiasmatic nucleus: the role of AMPA/KA glutamate receptors. *J. Neurophysiol.* **88**, 817–828 (2002).